Wetting of Inclined Nano-textured Surfaces by Self-healing Agents

Seongpil An,[1,2] Yong Il Kim,[2] Alexander L. Yarin,[1,2,]* Sam S. Yoon[2,]*

[1]*Department of Mechanical and Industrial Engineering, University of Illinois at Chicago, 842 W. Taylor St., Chicago IL 60607-7022, USA*

[2]*School of Mechanical Engineering, Korea University, Seoul 02841, Republic of Korea*

Abstract

Experiments were conducted to study spreading of droplets of liquid healing agents on tilted nanofiber mats, which is relevant in the framework of self-healing engineered materials with vascular networks. In the present situation the effect of gravity on drop spreading is important, as well as the inclination angle and the mat thickness. In the control case of gravity-driven spreading of droplets on an inclined polydimethylsiloxane (PDMS) surface the results agreed fairly well with the theoretical predictions in the framework of the lubrication theory for the intact surfaces. However, spreading on the inclined nanofiber mats revealed significant deviations from the theory due to the imbibition of liquid into the inter-fiber pores. The imbibition effect, which stems from the wettability-driven suction, increased as the mat thickness increased. Notably, the imbibition effect also increased as the inclination angle increased.

*Corresponding author: ayarin@uic.edu, skyoon@korea.ac.kr

Recently, a vascular self-healing approach has been proposed for various industrial applications as one of the most promising next-generation techniques aiming self-repairing engineered materials. In the framework of this approach the vascular core-shell fibers with healing agents in the core are embedded in a surrounding matrix forming self-healing durable composites.[1-13] The structure of the vascular system and the diameter of the embedded fibers can be controlled by means of various fabrication methods and manufacturing conditions.[14-25] To improve healing performance in the framework of the vascular self-healing approach, above all, the diameter of the embedded core-shell fibers needs to be reduced because the composite strength and resilience against delamination, as well as the releasing rate of the healing agents are improved as the cross-sectional diameter decreases.[26,27] Among numerous methods, co-electrospinning,[18,24,25] emulsion-electrospinning,[20,22,23] and solution blowing[28] techniques have successfully formed nano-scale core-shell-structured fibers.

An et al.[29] recently studied the physical mechanism of the self-healing process, in which healing agents spread over a porous horizontal polyacrylonitrile (PAN) nanofiber (NF) mats driven by wettability and elucidated the rate of coalescence of the resin monomer and cure droplets, which is the key element at play. In particular, they showed that thicker NF mats, which possessed a more developed porosity, facilitate the absorption of liquid agents, while reducing their wetted footprint at the surface. Here, we further explore wettability-driven spreading of liquid healing agents over the inclined NF mats where the gravity effect can be significant and affect drop coalescence in a more pronounced way.

Porous NF mats were fabricated by using electrospinning.[30-33] First, 8 wt% polyacrylonitrile (PAN, M_w = 150 kDa, Sigma-Aldrich) solution was prepared by dissolving PAN powder in dimethylformamide (DMF, 99.8%, Sigma-Aldrich) and magnetically stirring

2

for 1 day at room temperature. Next, the PAN solution was electrospun with an 18-gauge needle (Nordson EFD) equipped syringe, a syringe pump (Legato 101, KD Scientific), and a DC power supply (EL20P2, Glassman High Voltage). The flow rate of the solution was $Q = 800$ μl/h and an applied high DC voltage was $V = 12.5$ kV. The as-spun NFs were collected on a rotating drum. The angular speed of the drum was 200 rpm and the distance between the needle and the drum was 12 cm. Different NF mats of thicknesses (t_{NF}) of $t_{NF} = 33, 68$ and 135 μm were prepared by varying the electrospinning time (t_{es}), which had the average pore sizes of 0.64, 0.54, and 0.49 μm^2, respectively. The average pore size value of each NF mat was obtained by measuring 30 pores from 10 scanning electron microscopy (SEM) images.

A polydimethylsiloxane (PDMS) film was fabricated by blending dimethylvinyl-terminated dimethyl siloxane (resin) and methylhydrogen dimethyl siloxane (cure) liquids (i-Nexus) with the volume ratio of 10:1 and drying the blend for 2 days at room temperature. Note that these liquids were also used as siloxane-based healing agents in several the previous studies.[18,22-25,34-37]

Fig. 1 depicts a schematic of spreading of a self-healing droplet on an inclined flat PDMS film or on a porous NF mat. Several different inclination angles of $\theta = 30º, 45º, 60º$, and 70º were used in the experiments to observe the effect of the inclination on droplet spreading. The resin or cure liquid was supplied and dripped onto the substrates by a 23-gauge needle-equipped (Nordson EFD) syringe with a flow rate of $Q = 3$ μl/min. The distance between the needled and the point, where the droplet touched the inclined substrate, was 7.25 mm.

To capture images of spreading droplets, a high-speed camera (Vision Research) was used. A side-view of the contact length of the spreading droplet (l, cf. **Fig. 1**) was measured using ImageJ software (US National Institutes of Health). Viscosity (μ) was measured by

means of a rotational rheometer (DHR-1, TA Instrument, USA). Surface tension (σ) using a contact angle analyzer (Phoenix 300 Touch, SEO), which is based on the pendant drop method.[38-40]

Figs. **2(a)–2(d)** and **3(a)–3(d)** show the experimental results for the resin droplet spreading on a flat PDMS film and different NF mats at several inclination angles (θ) from 30º to 70º. In the all the inclination cases, the side-view contact line length l of the spreading droplets increased as time t increased. In the horizontal case $\theta = 0$º that was studied in our previous work,[29] the spreading resin droplet radii (a, which is the half of the l value in that case) on PDMS plane and the NF mat with thickness $h_{NF} = 33$ μm also increased as time t increased. However, note that, for on the thicker NF mats with $h_{NF} = 68$ and 135 μm at $\theta = 0$º,[29] the increase in a (and thus, in $l = 2a$) had ceased or a (and l) could even start to decrease because of the absorption of liquids by the thicker porous NF mats with significant pore volume. Similarly to the previous work, the enhanced imbibition into thicker mats was revealed here for all inclination angle values (**Figs. 2(a)–2(d)**). However, it never led to a decrease in l in time (**Figs. 2(a)–2(d)**). Furthermore, one can observe that the values of l increased for the same substrate as the inclination angle θ increased due to the enhanced downward gravity force along the surface. For example, for PDMS film at $t = 150$ s the value of l_{PDMS} increased from 7.9 to 14.3 mm and for the 68 μm film at $t = 300$ s the value of $l_{68\,\mu m}$ increased from 6.7 to 10.4 mm while the inclination angle increased from $\theta = 30$º to 70º.

Even though the values of the lengths l of the cure droplets were lower compared to the comparable cases of the resin droplets depicted in **Figs. 2(a)–2(d)**, similar trends were also observed in the experimental results for the cure droplets shown in **Figs. 2(e)–2(h)** and **3(e)–3(h)**. Note that the characteristic hydrodynamic time, $\tau_H = r\mu/\sigma$ (where r is the characteristic

4

radius of the pores between NFs in the mat),[29,41] of the cure ($\tau_{h, \text{cure}} = 1.4 \times 10^{-5}$ s) is relatively lower than that of the resin ($\tau_{h, \text{resin}} = 8.7 \times 10^{-4}$), which resulted in a higher imbibition rate of cure compared to that of the resin. Note that the value of r used for the estimate here is $r = 0.42$ µm, which is the average value obtained for different NF mats of thicknesses (t_{NF}) of $t_{NF} = 33$, 68 and 135 µm. For all inclination angles for the spreading cure droplets the side-view length l mostly increased in time, albeit with the tendency to saturation in the case of the thicker NF mats. This tendency was more pronounced for the cure droplets compared to the resin ones (cf. **Fig. 2**). Note also the anomalous behavior recorded for the cure droplets. Namely, the length of the side-view length $l_{68 \text{ µm}}$ in the interval $t = 2.0$–3.0 s was smaller at $\theta = 60°$ than at $\theta = 70°$ [cf. **Figs. 2(g) and 2(h)**]. Furthermore, the significantly different values of l on different substrates at $t = 0$ s were observed with the cure droplets in the case of $\theta = 70°$ (**Fig. 2(h)**), in distinction from the resin droplets (cf. **Figs. 2(d)**). This can be attributed to a combined effect of the low viscosity of the cure (**Table I**) and the high inclination angle, which caused an unstable initial sliding of the cure droplets. Note that such an instability of a droplet was further enhanced when the inclination angle increased up to $\theta = 80°$ (not shown here).

TABLE I. Viscosity and surface tension values of the resin and the cure liquids.

	μ (Pa·s)	σ (mN·m^{-1})
Resin	4.97	23.94
Cure	0.06	17.67

The capillary numbers (Ca = $\mu U / \sigma$) of the self-healing agents in the present work are relatively large (where μ and σ are the viscosity and surface tension, respectively, and U is the velocity of the lowest tip of the contact line), namely, Ca = $(7.5$–$8.8) \times 10^{-3}$. Accordingly, the spreading droplets on the NF mats can be considered as being viscosity-dominated rather than

capillarity-dominated.[42] In the previous work of the present group,[29] in the case with no inclination ($\theta = 0°$), the experimentally obtained values of the drop footprint radius a in the wettability-driven spreading resin and cure droplets on PDMS film and NF mats were compared with the Hoffman-Voinov-Tanner law valid for the intact perfectly wettable surfaces[29,37,43]

$$a = \left\{ 0.107 \frac{\sigma}{\mu} \left(\frac{4V}{\pi} \right)^3 t \right\}^{1/10} \propto t^{1/10} \tag{1}$$

where t is time, and the droplet volume $V = 4\pi a_0^3/3$, with a_0 being the volume-equivalent radius of the spreading droplet. The comparison showed that the data can disagree with **Eq. (1)** due to the imbibition of liquid into NF mats, with the deviation being more pronounced on the thicker mats.[29]

On the other hand, Huppert theoretically studied spreading of viscous fluid down a inclined surface and found the dependence of the length of its footprint on time in the form[44]

$$l_{Theo} = \left(\frac{9A^2 g \sin\theta}{4\nu} t \right)^{1/3} \tag{2}$$

where A and ν are the initial side-view cross-sectional area and the kinematic viscosity of liquid, and g is gravity acceleration. Note that the observed curvatures of the sliding droplet surfaces are relatively small,[44,45] which means that the surface tension effect can be neglected, as in **Eq. (2)**. This is corroborated by the present **Fig. 3** (especially, by the drop tails highlighted by red dotted lines in these figures). In **Fig. 4**, the experimental results (cf. **Fig. 2**) are compared with the theoretical predictions of **Eq. (2)** (the latter are shown by the orange dash lines in **Fig. 4**). Similarly to the previous work,[29] the comparisons which involve **Eq. (2)** exhibited a slight

6

discrepancy between the experimental and the theoretical results due to the uncertainty in the beginning of the asymptotic regime corresponding to **Eq. (2)**. To eliminate this uncertainty factors of 0.6 and 0.8 for the resin and cure droplets, respectively, were used as multipliers in **Eq. (2)**. Namely, the dependences of $0.6l_{Theo}$ and $0.8l_{Theo}$ were plotted in **Fig. 4**. These factors, obviously, cannot affect the scaling $l_{Theo} \sim t^{1/3}$ predicted by **Eq. (2)**.

Fig. 4 show the experimental vs. theoretical results for the spreading resin and cure droplets, respectively, on PDMS film and the NF mats of different thickness (h_{NF}) at different inclination angles θ. In all the cases of the resin droplets on PDMS film at different values of θ [**Fig. 4(a)–4(d)**], the theoretical scaling predicted by **Eq. (2)** agrees fairly well with the experimental data. However, in in the case of the NF mats, a significant decrease in the scaling exponent for l appears compared to the predictions of **Eq. (2)**, as the mat thickness h_{NF} increased. This stems from the imbibition of the resin liquid into NF mats.[29] In contrast to the resin droplets, the comparison for the cure droplets even on the PDMS films with different inclination angles θ already revealed slight differences [**Fig. 4(f)–4(h)**]. The overall slopes of the experimental dependences seemingly decreased even more compared to the scaling predicted by **Eq. (2)**, which is attributed to the lower viscosity of the cure compared to that of the resin (**Table I**), which enhances imbibition into thicker NF mats and also invalidates the viscosity-dominated lubrication approximation implied by **Eq. (2)**. Note that at large inclination angle $\theta = 70°$ case even the case of the PDMS film revealed a significant difference with predictions of **Eq. (2)** because of the unstable behavior of the spreading cure droplet (cf.

Section 3). **(R1-1, R1-2)** It should be emphasized that the majority of the experimental

dependencies shown in **Fig. 4**, in fact, deviate from a linear fit. Therefore, they cannot be described a power law, which is a direct consequence of the imbibition of the mats. Note also,

7

that the theory which describes the imbibition effect on drop spreading on nanofiber mats is currently available only for the case of zero inclination angle, $\theta = 0°$ (cf. **Ref. 29**).

In summary, gravity-driven spreading of healing agent droplets over inclined electrospun porous nanofiber mats revealed a significant wettability-driven imbibition effect, which is enhanced on thicker and/or more inclined mats. Due to this effect, Huppert's analytical solution used to estimate a droplet length in the direction of spreading on intact non-porous flat substrates is inapplicable in the present case. The imbibition effect observed in the present work is important for self-healing engineered materials with vascular nanofiber-based delivery structure, since their effective operation is determined, in part, by spreading distance of healing agents from the damaged location.
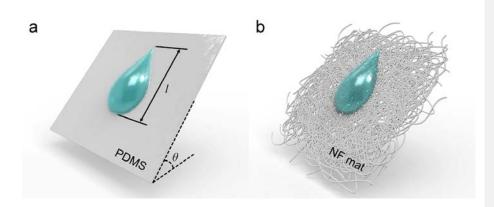
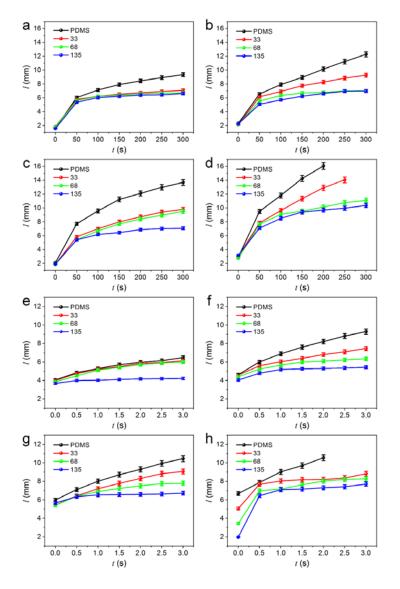## Acknowledgements

References

[1] D. Y. Wu, S. Meure, and D. Solomon, Prog. Polym. Sci. **33** (5), 479 (2008).

[2] M. Samadzadeh, S. H. Boura, M. Peikari, S. Kasiriha, and A. Ashrafi, Prog. Org. Coat. **68** (3), 159 (2010).

[3] B. Blaiszik, S. Kramer, S. Olugebefola, J. S. Moore, N. R. Sottos, and S. R. White, Annu. Rev. Mater. Res. **40**, 179 (2010).

[4] M. D. Hager, P. Greil, C. Leyens, S. van der Zwaag, and U. S. Schubert, Adv. Mater. **22** (47), 5424 (2010).

[5] W. H. Binder, *Self-healing polymers: from principles to applications*. (John Wiley & Sons, 2013).

[6] Y. Yang and M. W. Urban, Chem. Soc. Rev. **42** (17), 7446 (2013).

[7] Z. Wei, J. H. Yang, J. Zhou, F. Xu, M. Zrínyi, P. H. Dussault, Y. Osada, and Y. M. Chen, Chem. Soc. Rev. **43** (23), 8114 (2014).

[8] Y. Yang, X. Ding, and M. W. Urban, Prog. Polym. Sci. **49**, 34 (2015).

[9] X. K. Hillewaere and F. E. Du Prez, Prog. Polym. Sci. **49**, 121 (2015).

[10] H. Wei, Y. Wang, J. Guo, N. Z. Shen, D. Jiang, X. Zhang, X. Yan, J. Zhu, Q. Wang, and L. Shao, J. Mater. Chem. A **3** (2), 469 (2015).

[11] V. K. Thakur and M. R. Kessler, Polym. **69**, 369 (2015).

[12] C. E. Diesendruck, N. R. Sottos, J. S. Moore, and S. R. White, Angew. Chem., Int. Ed. **54** (36), 10428 (2015).

[13] M. Behzadnasab, S. Mirabedini, M. Esfandeh, and R. Farnood, Prog. Org. Coat. **105**, 212 (2017).

9

[14]M. Stratmann, A. Leng, W. Fürbeth, H. Streckel, H. Gehmecker, and K.-H. Groβe-Brinkhaus, Prog. Org. Coat. **27** (1-4), 261 (1996).

[15]S. M. Bleay, C. B. Loader, V. J. Hawyes, L. Humberstone, and P. T. Curtis, Composites, Part A **32** (12), 1767 (2001).

[16]J. W. C. Pang and I. P. Bond, Compos. Sci. Technol. **65** (11), 1791 (2005).

[17]K. S. Toohey, N. R. Sottos, J. A. Lewis, J. S. Moore, and S. R. White, Nat. Mater. **6** (8), 581 (2007).

[18]J. H. Park and P. V. Braun, Adv. Mater. **22** (4), 496 (2010).

[19]J. F. Patrick, N. R. Sottos, and S. R. White, Polym. **53** (19), 4231 (2012).

[20]S. Sinha-Ray, D. D. Pelot, Z. P. Zhou, A. Rahman, X.-F. Wu, and A. L. Yarin, J. Mater. Chem. **22** (18), 9138 (2012).

[21]S. R. White, J. S. Moore, N. R. Sottos, B. P. Krull, W. A. Santa Cruz, and R. C. R. Gergely, Science **344** (6184), 620 (2014).

[22]M. W. Lee, S. An, C. Lee, M. Liou, A. L. Yarin, and S. S. Yoon, J. Mater. Chem. A **2** (19), 7045 (2014).

[23]M. W. Lee, S. An, C. Lee, M. Liou, A. L. Yarin, and S. S. Yoon, ACS Appl. Mater. Interfaces **6** (13), 10461 (2014).

[24]S. An, M. Liou, K. Y. Song, H. S. Jo, M. W. Lee, S. S. Al-Deyab, A. L. Yarin, and S. S. Yoon, Nanoscale **7** (42), 17778 (2015).

[25]T. Q. Doan, L. S. Leslie, S. Y. Kim, R. Bhargava, S. R. White, and N. R. Sottos, Polym. **107**, 263 (2016).

[26]A. Kousourakis and A. Mouritz, Smart Mater. Struct. **19** (8), 085021 (2010).

[27]S. Sinha-Ray, M. W. Lee, S. Sinha-Ray, S. An, B. Pourdeyhimi, S. S. Yoon, and A. L. Yarin, J. Mater. Chem. C **1** (21), 3491 (2013).
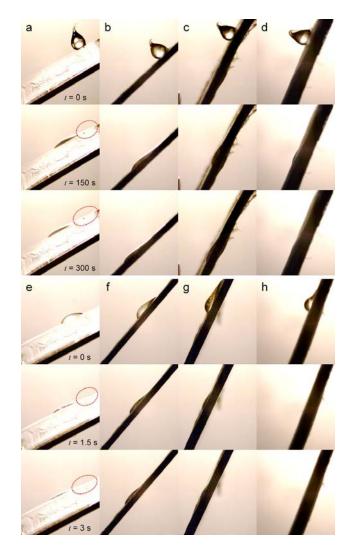
10

[28]M. W. Lee, S. S. Yoon, and A. L. Yarin, ACS Appl. Mater. Interfaces **8** (7), 4955 (2016).

[29]S. An, Y. I. Kim, M. W. Lee, A. L. Yarin, and S. S. Yoon, Langmuir **33** (40), 10663 (2017).

[30]S. A. Theron, E. Zussman, and A. L. Yarin, Polym. **45** (6), 2017 (2004).

[31]D. H. Reneker and A. L. Yarin, Polym. **49** (10), 2387 (2008).

[32]M. W. Lee, S. An, S. S. Latthe, C. Lee, S. Hong, and S. S. Yoon, ACS Appl. Mater. Interfaces **5** (21), 10597 (2013).

[33]S. An, H. S. Jo, K. Y. Song, M. G. Mali, S. S. Al-Deyab, and S. S. Yoon, Nanoscale **7** (45), 19170 (2015).

[34]M. W. Lee, S. An, H. S. Jo, S. S. Yoon, and A. L. Yarin, ACS Appl. Mater. Interfaces **7** (35), 19555 (2015).

[35]M. W. Lee, S. An, H. S. Jo, S. S. Yoon, and A. L. Yarin, ACS Appl. Mater. Interfaces **7** (35), 19546 (2015).

[36]M. Lee, S. Sett, S. An, S. S. Yoon, and A. L. Yarin, ACS Appl. Mater. Interfaces **9** (32), 27223 (2017).

[37]M. Lee, S. S. Yoon, and A. L. Yarin, ACS Appl. Mater. Interfaces **9** (20), 17449 (2017).

[38]C. E. Stauffer, J. Phys. Chem. **69** (6), 1933 (1965).

[39]F. Hansen and G. Rødsrud, J. Colloid Interface Sci. **141** (1), 1 (1991).

[40]C. Dry, Compos. Struct. **35** (3), 263 (1996).

[41]U. Stachewicz, J. F. Dijksman, D. Burdinski, C. U. Yurteri, and J. C. Marijnissen, Langmuir **25** (4), 2540 (2009).

[42]P. Ringrose and M. Bentley, in *Reservoir Model Design* (Springer, 2015), pp. 115.

[43]J. Berg, *Wettability*. (Taylor & Francis, New York, 1993).

[44]H. E. Huppert, Nature **300** (5891), 427 (1982).

[45]S. Reznik and A. Yarin, Phys. Fluids **14** (1), 118 (2002).
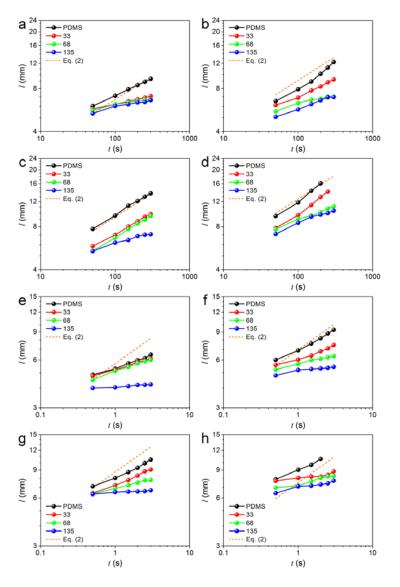
11

FIG. 1. Schematic of the wetting experiments with resin or cure droplets on (a) an inclined flat PDMS film and (b) an inclined porous NF mat.

FIG. 2. Contact length of droplet l as a function of time t and the inclination angle θ for (a–d) the resin and (e–h) the cure droplets spreading on the PDMS film and the NF mats with thicknesses h_{NF} = 33, 68, and 135 μm: (a, e) θ = 30°, (b, f) θ = 45°, (c, g) θ = 60°, and (d, h) θ = 70°.

FIG. 3. Side-view images of spreading (a–d) resin and (e–h) cure droplets at different time moments on different substrates at different inclination angles θ: (a, e) PDMS film at $\theta = 30°$, (b, f) NF mat with $h_{NF} = 33$ μm at $\theta = 45°$, (c, g) NF mat with $h_{NF} = 68$ μm at $\theta = 60°$, and (d, h) NF mat with $h_{NF} = 135$ μm at $\theta = 70°$. The red dotted lines highlight droplet tails. The green lines in (b) show how to measure the contact length l.

FIG. 4. Comparison of the experimental and theoretical results for the contact length l as a function of time t for (a–d) the resin and (e–h) the cure droplets on PDMS film and the NF mats at different inclinations: (a, e) $\theta = 30°$, (b, f) $\theta = 45°$, (c, g) $\theta = 60°$, and (d, h) $\theta = 70°$.